Compressed sensing sparse reconstruction for coherent field imaging*

Bei Cao(曹蓓)†, Xiu-Juan Luo(罗秀娟), Yu Zhang(张羽), Hui Liu(刘辉), and Ming-Lai Chen(陈明徕)

Xi'an Institute of Optics and Precision Mechanics, Chinese Academy of Sciences, Xi'an 710119, *China*

(Received 6 November 2015; revised manuscript received 22 December 2015; published online 20 February 2016)

Return signal processing and reconstruction plays a pivotal role in coherent field imaging, having a significant influence on the quality of the reconstructed image. To reduce the required samples and accelerate the sampling process, we propose a genuine sparse reconstruction scheme based on compressed sensing theory. By analyzing the sparsity of the received signal in the Fourier spectrum domain, we accomplish an effective random projection and then reconstruct the return signal from as little as 10% of traditional samples, finally acquiring the target image precisely. The results of the numerical simulations and practical experiments verify the correctness of the proposed method, providing an efficient processing approach for imaging fast-moving targets in the future.

Keywords: coherent field imaging, computational imaging, sparse reconstruction, compressed sensing

PACS: 07.05.Hd, 43.60.Hj, 07.05.Tp **DOI:** 10.1088/1674-1056/25/4/040701

1. Introduction

Coherent field imaging, also referred to as a Fourier telescope (FT), is a novel and promising active imaging technique, having the potential to achieve high resolution images for satellite targets as far as geosynchronous target ranges.[1,2] In contrast to traditional imaging techniques, coherent field imaging is capable of imaging the targets through atmospheric turbulence, and the imaging quality is immune to downlink the turbulence effect[3,4] and optical quality of the receiver. It has therefore drawn considerable attention in recent years, becoming a promising candidate in the field of space surveillance and object recognition.[5,6]

Based on the computational imaging principle, coherent field imaging can produce good images from the target spatial frequency components encoded in the temporal signal reflected from the target, therefore return signal processing and reconstruction is essentially significant in the whole imaging system. By fine recovery and reconstruction of the return signal, the target image can be obtained with high resolution. At present, researchers have introduced some feasible approaches to improve the performance of return signal processing.[7,8] However, these methods are generally based on a requirement for sampling all the complete information about the return signal in data acquisition. If the inherent characteristic of the signal itself is considered, a more efficient processing scheme can be obtained.

Compressed sensing (CS) is a novel mathematical theory for sampling and reconstructing signals in an efficient way.[9] The CS has been previously reported in single-pixel imaging,[10] radar imaging,[11] and inline single-shot holography for tridimensional imaging.[12]

According to the analysis of sparsity for the return signal, we propose a genuine CS-based sparse reconstruction (CS-SR) scheme for coherent field imaging. Firstly, the sparse factor of the received signal is determined, then an effective random projection is implemented to greatly reduce the number of samples required in data acquisition, hence recovering the return signal from as little as 10% of random measurements, finally achieving the reconstructed image with high precision. The simulations and practical experiments prove the validity of CS-SR, developing an efficient processing approach for coherent field imaging in the applications of imaging fast-moving targets.

2. Principle of coherent field imaging

2.1. Imaging principle

Coherent field imaging is an active imaging technique based on computational imaging theory, which uses multiple beams from spatially separated transmitters to illuminate a distant target. Based on the spatial-temporal coding principle, the target spatial frequency components are encoded in the temporal signal reflected from the target. By collecting the return signal in the receiver and eliminating random atmospheric phase errors in the uplink turbulence by phase closure, the true amplitude and phase of the target can be recovered and processed to reconstruct the target image. The schematic diagram of the imaging principle is shown in the following figure (Fig. 1).

*Project supported by the National Natural Science Foundation of China (Grant No. 61505248) and the Fund from Chinese Academy of Sciences, the Light of "Western" Talent Cultivation Plan "Dr. Western Fund Project" (Grant No. Y429621213).

†Corresponding author. E-mail: candy@opt.ac.cn

© 2016 Chinese Physical Society and IOP Publishing Ltd

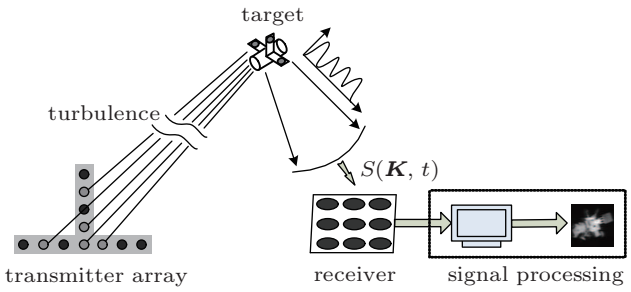


Fig. 1. (color online) Schematic diagram of coherent field imaging.

The return signal $S(\boldsymbol{K},t)$ in the time-domain can be formulated as follows:

$$S(\boldsymbol{K},t) = cN_{\mathrm{b}}ITO(\boldsymbol{K}=0)|_{f_x,f_y=0} + cIT\sum_{n=0}^{N_{\mathrm{b}}-1}\sum_{m=n+1}^{N_{\mathrm{b}}-1} O(\boldsymbol{K}_{nm}) \times \exp[\mathrm{i}(\Delta\omega_{mn}(t+T/2)+\phi_{m,n})] + \mathrm{c.c}, \quad (1)$$

where N_{b} denotes the number of beams transmitted at the same moment, $\boldsymbol{K}$ is the optical wave number of the transmitted light, I is the intensity of the transmitted wave at the object plane, $\Delta\omega_{mn}$ is the beat frequency formed by the transmitted beams m and n, $\phi_{mn}=\phi_m-\phi_n$ is an initially unknown gross-piston phase difference between the m and n beams, $O(\boldsymbol{K}_{nm})$ is the target spatial component in spatial frequency $\boldsymbol{K}_{nm}=(f_x,f_y)$. By sampling the return signal in each baseline location to acquire the whole Fourier spectrum of the target, the target profile $O(x,y)$ can be reconstructed by inverse FFT

$$O(x,y)=\iint O(f_x,f_y)\cdot\exp[\mathrm{i}2\pi(f_x x+f_y y)]\,\mathrm{d}f_x\,\mathrm{d}f_y.$$

2.2. Traditional return signal processing

The traditional return signal processing is realized under the constraint of the Nyquist sampling theorem. All the complete information about the received signal needs to be sampled for extracting the important spectrum information providing for the next image reconstruction. However, in the applications for imaging fast-moving objects, the imaging time is a crucial issue. It will be favorable to accelerate the processing efficiency of data acquisition. From this angle, we are to explore a novel and efficient processing scheme to provide a better solution.

3. CS-based sparse signal reconstruction

3.1. Sparsity analysis

Based on the imaging principle of coherent field imaging, if the return signal is sparse and compressible, it is possible to realize a more efficient way in the process of signal processing. CS is a novel signal processing theory that allows data reconstruction with fewer samples than traditionally required. As long as the original signal is sparse in some basis, it is possible to recover N pieces of information in object space from $M \ll N$ incoherent measurements with high confidence.

We firstly analyze the characteristic of the return signal. By illuminating a target with a fringe pattern that sweeps across it due to frequency differences between laser beams, the received signal in the time domain is a linear combination of several cosine signals. Therefore we transform the return signal into the Fourier spectrum domain to reveal that it is sparse and satisfies the precondition for applying CS. Fourier transform is used as a sparse basis matrix, then an $N\times 1$ original return signal $S(\boldsymbol{K},t)$ can be represented more efficiently in $\boldsymbol{\Psi}$ domain as follows:

$$S(\boldsymbol{K},t)=\sum_{i=1}^{N}\alpha_i\psi_i \quad \text{or} \quad S(\boldsymbol{K},t)=\boldsymbol{\Psi}\boldsymbol{\alpha}, \quad (2)$$

where $\boldsymbol{\Psi}=[\psi_1|\psi_2|\cdots|\psi_N$ is the $N\times N$ orthonormal discrete Fourier transform basis matrix; $\boldsymbol{\alpha}$ is the $N\times 1$ column vector of weighting coefficients, as an equivalent representation of $S(\boldsymbol{K},t)$ in $\boldsymbol{\Psi}$ domain; only K values of the α_i coefficients are nonzero and $(N-K)$ are zero, $S(\boldsymbol{K},t)$ is K-sparse and sparse factor can be defined as $K=C_{N_{\mathrm{b}}}^2$, which is determined by the number of formed beat frequencies at the same moment.

3.2. Realization of CS-SR

According to the condition that the received signal is compressible, instead of sampling the entire data, we perform a compressed data acquisition under CS theory and put forward a novel CS-SR scheme for signal processing in coherent field imaging. The realization of CS-SR includes two steps: random projection and sparse reconstruction.

The measurement process is formulated as

$$\boldsymbol{y}=\boldsymbol{\Phi}S(\boldsymbol{K},t)=\boldsymbol{\Phi}\boldsymbol{\Psi}\boldsymbol{\alpha}=\boldsymbol{\Theta}\boldsymbol{\alpha}, \quad (3)$$

where $\boldsymbol{\Phi}$ is an $M\times N$ measurement matrix, by substituting Eq. (2) into Eq. (3), we obtain an $M\times N$ CS matrix $\boldsymbol{\Theta}=\boldsymbol{\Phi}\boldsymbol{\Psi}$, which can project the sparse coefficient vector $\boldsymbol{\alpha}$ to the $M\times 1$ measurement vector $\boldsymbol{y}$. To guarantee that no important information is damaged in the dimensionality reduction process, for some constant $0<\delta_K<1$, $\boldsymbol{\Theta}$ should satisfy the restricted isometry property (RIP) rule:[13]

$$(1-\delta_K)\|\boldsymbol{\alpha}\|_2^2 \le \|\boldsymbol{\Theta}\boldsymbol{\alpha}\|_2^2 \le (1+\delta_K)\|\boldsymbol{\alpha}\|_2^2. \quad (4)$$

We select $\boldsymbol{\Phi}$ as a random matrix, an identically distributed Gaussian measurement matrix, and set $M \ge cK\log(N/K)$ as the dimension of the random measurements, with c being a small constant, in that case, $\boldsymbol{\Phi}$ is incoherent with the sparse basis matrix $\boldsymbol{\Psi}$, thus the RIP rule can be achieved with high probability.

By the above random projection process, the number of the return signal samples can be greatly reduced from $\boldsymbol{R}^N$ to $\boldsymbol{R}^M$, $M \ll N$. In what follows we employ an iterative OMP algorithm [14] to carry out an optimized data recovery from a few sparse samples. The reconstruction process is implemented by

$$\begin{aligned} &\hat{\boldsymbol{\alpha}} = \text{argmin} \left\| \boldsymbol{\alpha}' \right\|_1 \quad \text{such that} \\ &\boldsymbol{\Theta}\boldsymbol{\alpha}' = \boldsymbol{y} \quad \text{then} \quad \hat{S}(\boldsymbol{K},t) = \boldsymbol{\Psi}\hat{\boldsymbol{\alpha}}. \end{aligned} \tag{5}$$

The reconstruction error is defined as the form: $e = \text{norm}(\hat{S} - S)/\text{norm}(S)$, where S is the original return signal, $\hat{S}$ represents the reconstructed signal, and norm$(\times)$ denotes the norm operation. The error e can be reduced by properly choosing M and iteration times of the reconstruction process.

At the end, based on the reconstructed return signal, a robust all-phase FFT target reconstruction algorithm[15] is used to reconstruct the target image. The realization chart is shown in Fig. 2. The sparse factor of $S(\boldsymbol{K},t)$ is first determined, then the random measurement matrix is designed to greatly reduce the required samples. Finally the original signal is reconstructed with high precision by correctly setting the value of M and iteration times.

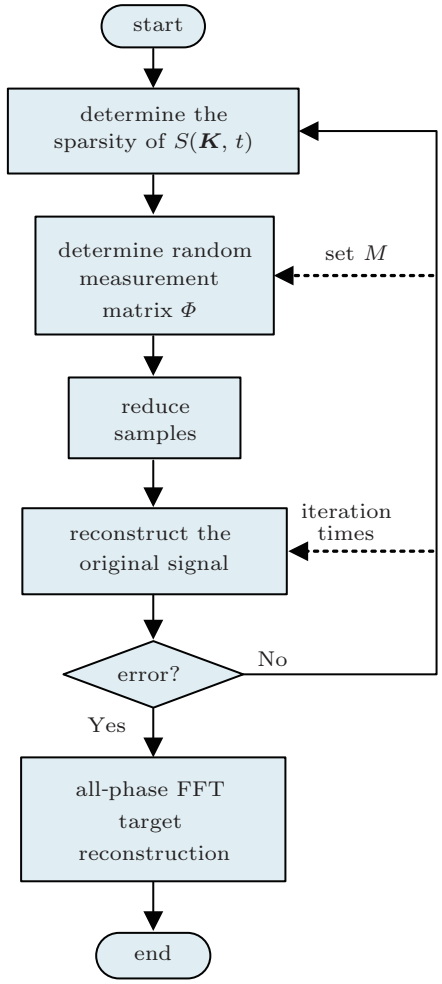


Fig. 2. (color online) Realization chart of CS-SR scheme.

4. Results and discussion

In this section, we present both the numerical simulations and the practical measurements to verify the validity of the CS-SR scheme by comparison with the traditional reconstruction (TR) scheme.

The basic parameters of the coherent field imaging system are set as follows: the wavelength of the laser is 1064 nm, the imaging distance is 60 m, the target size is 4 mm; the T-type transmitter array is adopted and three beams are transmitted simultaneously at the same moment. The demonstration of the baseline location is shown in Fig. 3. N_a is the total number of apertures in each u axis and v axis. The procedure of data sampling starts from $(2,0)$ to $(N_\text{a}, 0)$ in the u axis, $(0,2)$ to $(0, N_\text{a})$ in the v axis. By properly setting the modulated frequencies among three beams, the target spectra in the coordinates can be correctly extracted.

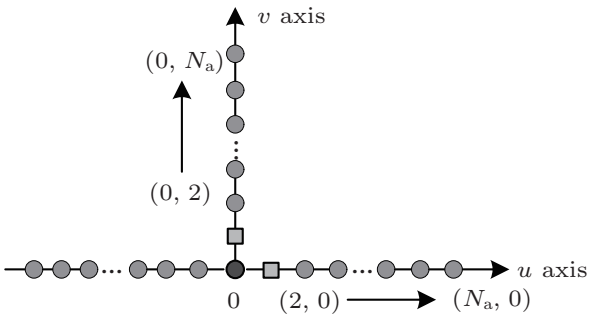


Fig. 3. (color online) Demonstration of baseline configuration in T-type array.

4.1. Numerical simulations

We numerically simulate the intensity accumulation of the return signal at the object plane by receiving and processing the return signal to reconstruct the target image. In the simulations, the modulated frequencies among three beams are chosen to be $[0,1,3] \times 10$ kHz, and the sampling rate is 1 MHz, sampling 500 samples in each baseline location.

4.1.1. Sparse signal reconstruction in ideal environment

Firstly, we verify the signal reconstruction precision of CS-SR in an ideal environment. The signal-to-noise (SNR) level is set to be 200 dB. In the CS-SR scheme, the dimension of random measurements should satisfy $M \geq 22$, which is a least requirement under the condition of sparse factor $K = 3$. We set $M = 23$ and $M = 44$ to separately reconstruct the return signal, and iteration times are set to be 4, i.e., 4 times sparse factor. The reconstruction error in the u axis sampling is computed and listed in Table 1.

As Table 1 indicates, when we set $M = 23$, the number of random measurements just meets the minimal value that the RIP rule desires. In this case the reconstruction error is not

very stable, having some big value beyond the expectation, such as at the locations $(4,0)$, $(5,0)$, and $(6,0)$. In order to achieve better performance, we increase the number of measurements to $M = 44$ with constant $c = 2$; as a result, the error is effectively reduced and keeps stable around $\times 10^{-10}$ level at each baseline location.

Table 1. Reconstruction errors of CS-SR in u-axis sampling ($N_a = 8$).

Location	(2, 0)	(3, 0)	(4, 0)	(5, 0)	(6, 0)	(7, 0)	(8, 0)
$M = 23$	1.63×10^{-10}	1.55×10^{-10}	0.248	0.117	0.111	1.60×10^{-10}	0.019
$M = 44$	1.26×10^{-10}	1.25×10^{-10}	1.31×10^{-10}	1.17×10^{-10}	1.16×10^{-10}	1.29×10^{-10}	1.20×10^{-10}

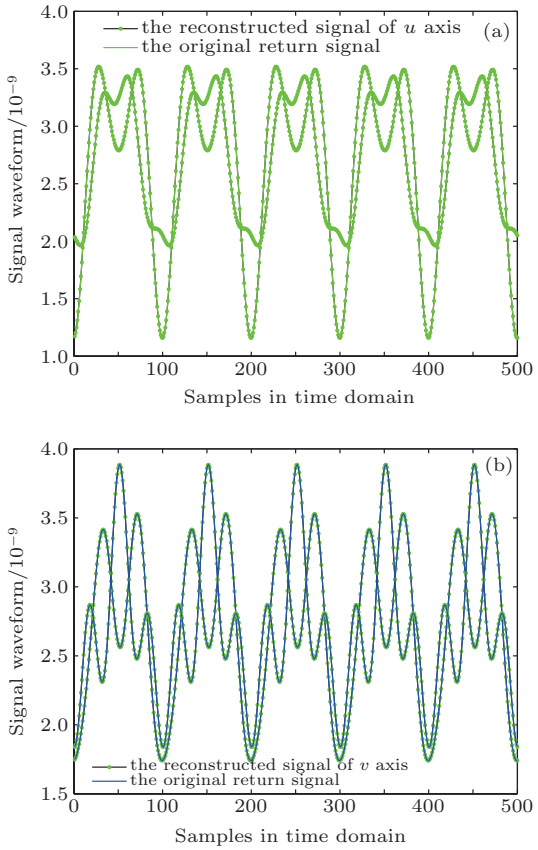


Fig. 4. (color online) Reconstructed return signals of CS-SR: (a) u axis data sampling; (b) v axis data sampling.

Figure 4 shows the original return signal and the reconstructed signal by CS-SR in the case of $M = 44$. For clarity, the waveforms at two baseline locations of u axis sampling and v axis sampling are plotted in Figs. 4(a) and 4(b), respectively. It is indicated that the reconstructed signal by CS-SR perfectly matches the original signal, that is to say, CS-SR can precisely reconstruct the return signal from as little as 8.8% of the samples that TR requires, thus greatly reducing the required sampling quantity in data acquisition. The reconstruction performance in the coordinate sampling is good as well; owing to the limited space in this paper, we do not plot them.

According to the reconstructed return signal by CS-SR, we reconstruct the target image by all-phase FFT reconstruction and compare the results with those of TR. Figure 5(a) is a simulated target, setting $N_a = 10$ and $N_a = 20$, figures 5(b) and 5(d) show the separately reconstructed target image by TR, and figures 5(c) and 5(e) show the corresponding results obtained by CS-SR respectively.

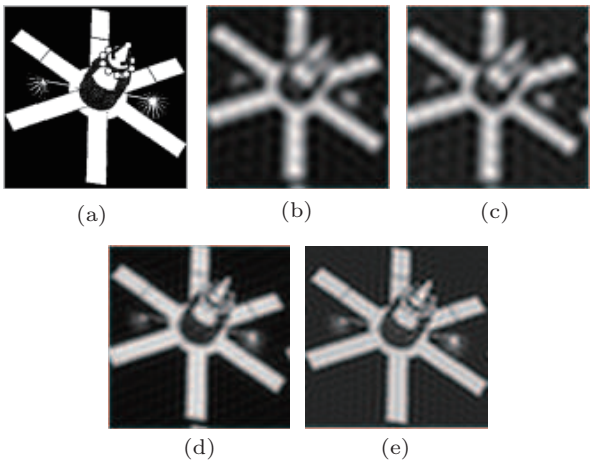


Fig. 5. Comparison among the reconstructed images: (a) simulated target 1; (b) the reconstructed image by TR ($N_a = 10$); (c) the reconstructed image by CS-SR ($N_a = 10$); (d) the reconstructed image by TR ($N_a = 20$); (e) the reconstructed image by CS-SR ($N_a = 20$).

As figure 5 demonstrates, the feasibility of the CS-SR scheme is proved, and the scheme is capable of reconstructing the target image with much fewer random samples ($M = 44$), less than 10% of that which the TR requires, while it still achieves as good image quality as TR. The analysis of the advantage of CS-SR shows that the CS-SR relies on the fact that the essential property of the return signal is effectively explored, which makes it possible to evidently reduce the sampling quantity under the CS processing framework. Based on the signal reconstructed with high accuracy, the quality of the reconstructed image can still be well maintained. The following simulations in a noise environment can further confirm this point.

4.1.2. Sparse signal reconstruction in noise environment

To test the reconstruction performance of CS-SR in a noise environment, we add white Gaussian noise to the simulated return signal and set different SNR levels. Referring to the situation of an ideal environment, we set the random measurements of CS-SR, i.e., $M = 44$ and $M = 66$. The reconstruction errors of u-axis sampling and v-axis sampling at each baseline location are shown in Figs. 6(a) and 6(b), respectively.

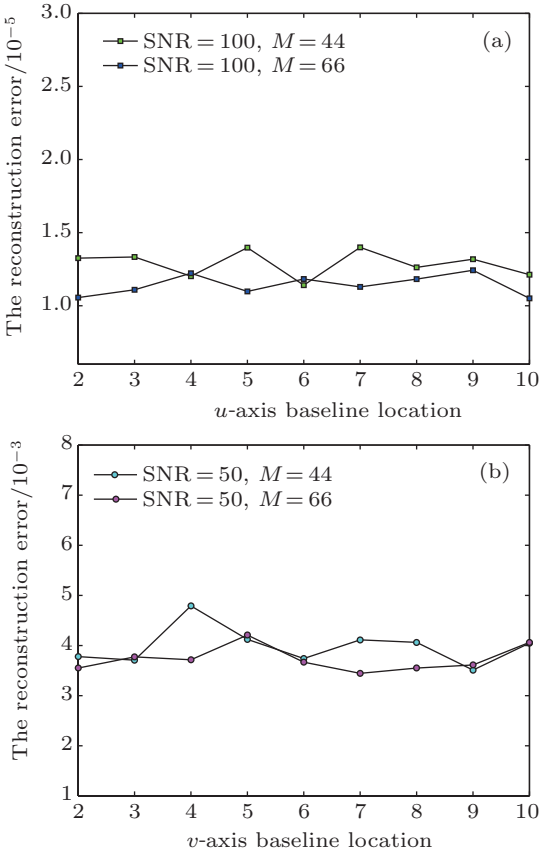


Fig. 6. (color online) Reconstruction errors: (a) u-axis sampling; (b) v-axis sampling.

As shown in Fig. 6, relatively high SNR can produce a better recovery precision, while increasing the number of random measurements can reduce the reconstruction error in the same SNR condition. In the situation of SNR = 100, M= 66, considering a simulated target 2 in more detail, we use the CS-SR and TR to reconstruct the target image, and the results are shown in Figs. 7(a)–7(e).

According to the above results, in order to obtain satisfactory reconstructed quality in a noise environment with low SNR, it is necessary to increase the number of random measurements in the CS-SR scheme. The quantity of the required samples is still much less than TR desires, which indicates that the determination of the sparse factor is a key issue in sparse reconstruction for coherent field imaging. Combined with the correct selection of measurement dimension, CS-SR can achieve good reconstruction performance even in a noisy environment.

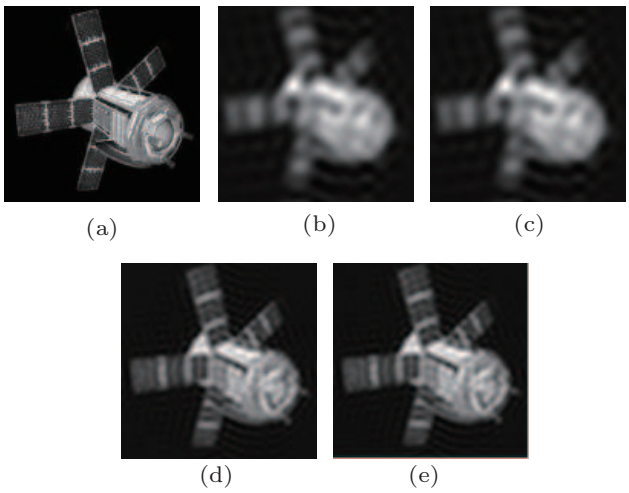


Fig. 7. Comparison among the reconstructed images: (a) simulated target 2; (b) the reconstructed image by TR ($N_a = 10$); (c) the reconstructed image by CS-SR ($N_a = 10$); (d) the reconstructed image by TR ($N_a = 20$); (e) the reconstructed image by CS-SR ($N_a = 20$).

4.2. Experimental results

The effectiveness of CS-SR is validated by the numerical simulations in Subsection 4.1. Then we apply CS-SR to an outdoor imaging system for the return signal processing and reconstruction.[15] Three different transmissive targets are adopted and a T-type array baseline scale is set to be 15×16. The modulated frequencies between three beams are chosen to be 0, 50 kHz, and 150 kHz respectively, and the sampling rate is 4 MHz.

We sample 4000 data points by TR at each baseline location. In terms of the outdoor SNR level, the measurement is in a range of 50 dB–70 dB; we set different values of random measurements in CS-SR and observe the reconstruction errors. According to the basic RIP rule, the dimensions of measurements should satisfy $M \geq 31$. Therefore, we first set the initial value of random samples to be M= 62. The random projection measurement is implemented with the Gaussian random matrix by directly projecting the original samples to the measurement space and making sure that no important frequency information is damaged in the projection process. Based on the CS-SR scheme, the mean value $\bar{e}$ and standard deviation δ of the reconstruction error are separately computed for each target, and the results are listed in Table 2.

Table 2. Reconstruction errors computed for three targets.

M		62	100	300	500	800	1000
Target S	$\bar{e}$	0.2128	0.0977	0.0832	0.0699	0.0682	0.0655
	δ	0.0105	0.0085	0.0076	0.0053	0.0046	0.0047
Target A	$\bar{e}$	0.1438	0.0659	0.0511	0.0475	0.0455	0.0448
	δ	0.0072	0.0057	0.0023	0.0027	0.0023	0.0021
Target six	$\bar{e}$	0.1335	0.0896	0.0759	0.0591	0.0585	0.0537
	δ	0.0092	0.0071	0.0055	0.0043	0.0036	0.0026

It is revealed from Table 2 that the reconstruction error decreases gradually as the number of random measurements, M, increases. Under the condition of $M \geq 500$, the mean $\bar{e}$ declines to a stable small value. Therefore, we choose and explore a lot more random measurements in a practical noise environment to guarantee a stable and accurate reconstruction performance. In that case, the total sampling number of CS-SR is still as little as $1/8$ that of traditional samples by TR. The standard deviation δ keeps steady in the reconstruction process, which indicates the stability of CS-SR realization.

According to experimental data, we set iteration times to be six times sparse factor to ensure a fast convergence in the reconstruction process. Considering the following three kinds of targets, the reconstructed images by TR and CS-SR with $M = 500$ are shown respectively in Figs. 8(a)–8(f).

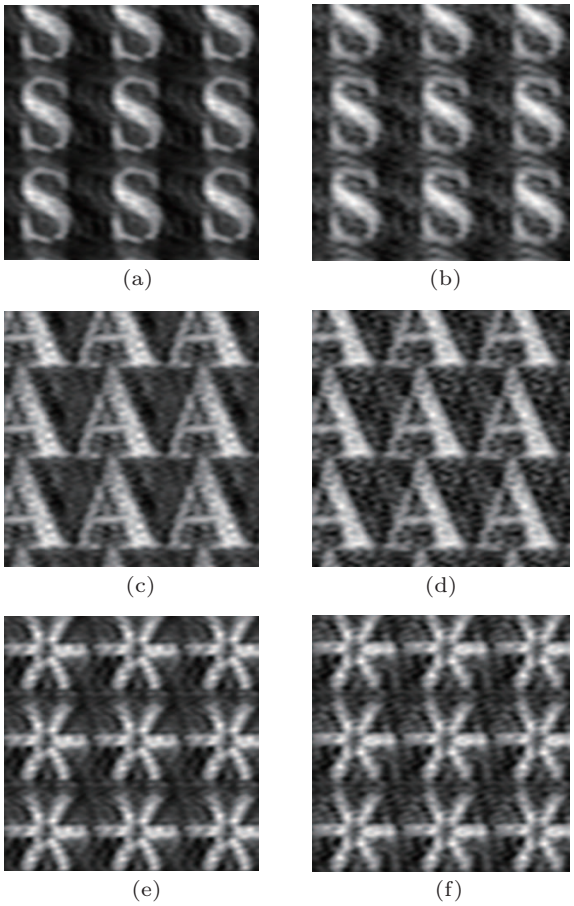


Fig. 8. Reconstructed images based on experimental data: (a) the reconstructed target S by TR; (b) the reconstructed target S by CS-SR; (c) the reconstructed target A by TR; (d) the reconstructed target A by CS-SR; (e) the reconstructed target six by TR; (f) the reconstructed target six by CS-SR.

Figure 8 proves the effectiveness of CS-SR in an outdoor imaging system. Based on the experimental data, CS-SR can achieve imaging quality almost as good as TR. According to Ref. [16], we compute the Strehl value of the reconstructed image to give a comparative analysis between CS-TR and TR in actual experiments. The Strehl values of Figs. 8(a)–8(f) are listed in Table 3.

Table 3. Image Strehl values of Fig. 8.

Fig. 8	(a)	(b)	(c)	(d)	(e)	(f)
Strehl value	0.8413	0.7261	0.7927	0.7075	0.8360	0.7342

The Strehl values of the reconstructed image by CS-SR are slightly lower than those of TR. For that the precision of signal reconstruction is not so high as that in the simulations considering the existence of noises in a practical outdoor environment. Nevertheless the target is still clearly recognizable. Therefore, the proposed CS-SR scheme provides an efficient means to enhance the sampling efficiency in data acquisition for coherent field imaging.

5. Conclusions

In this paper, we present a genuine CS-SR scheme for coherent field imaging. Based on the analysis result that the received signal is sparse and compressible, we accomplish effective random projection to greatly reduce the required samples in data acquisition, and finally reconstruct the return signal with high accuracy by much fewer measurements. The effectiveness of the CS-SR scheme is validated by simulations and practical experiments, showing that the CS-SR scheme provides an efficient signal processing approach and promoting the applications of coherent field imaging in fast-moving target imaging.

References

[1] Holmes R B, Ma S, Bhowmik A and Greninger C 1996 *J. Opt. Soc. Am. A* **13** 351
[2] Holmes R B and Brinkley T 1999 *Proc. SPIE* **3815** 11
[3] Lu L, Ji X L, Deng J P and Li X Q 2014 *Chin. Phys. B* **23** 064209
[4] Qian X M, Zhu W Y and Rao R Z 2015 *Chin. Phys. B* **24** 044201
[5] Stapp J, Spivey B, Chen L, Leon L, Hughes K, Sandler D and Cuellar E L 2006 *Proc. SPIE* **6307** 630701
[6] Cuellar E L, Cooper J, Mathis J and Fairchild P 2008 *Proc. SPIE* **7094** 70940G
[7] Yu S H, Wang J L, Dong L, Liu X Y and Wang G C 2013 *Acta Opt. Sin.* **33** 0811001 (in Chinese)
[8] Dong L, Liu X Y, Liu J and Yu S H 2013 *Acta Photon. Sin.* **42** 447 (in Chinese)
[9] Donoho D L 2006 *IEEE Trans. Inform. Theory* **52** 1289
[10] Duarte M F, Davenport M A, Takhar D, Laska J N, Sun T, Kelly K F and Baraniuk R G 2008 *IEEE Signal Processing Magazine* **25** 83
[11] Baraniuk R G and Steeghs P 2007 *IEEE Radar Conference*, April, 2007, Waltham, MA, USA, pp. 128–133
[12] Brady D, Choi K, Marks D, Horisaki R and Lim S 2009 *Opt. Express* **17** 13040
[13] Cand'es E J and Romberg J 2007 *Inverse Probl.* **23** 969
[14] Tropp J A and Gilbert A C 2007 *IEEE Trans. Inform. Theory* **53** 4655
[15] Cao B, Luo X J, Chen M L and Zhang Y 2015 *Acta Phys. Sin.* **64** 124205 (in Chinese)
[16] Cuellar E L, Stapp J and Cooper J 2005 *Proc. SPIE* **5896** 58960D